The International Journal of Biochemistry & Cell Biology 81 (2016) 223–232

Contents lists available at ScienceDirect

The International Journal of Biochemistry & Cell Biology

journal homepage: www.elsevier.com/locate/biocel

Quantitative extracellular matrix proteomics to study mammary and liver tissue microenvironments

Erica T. Goddard[a,1], Ryan C. Hill[b,1], Alexander Barrett[b], Courtney Betts[a], Qiuchen Guo[a], Ori Maller[c], Virginia F. Borges[d,e,f], Kirk C. Hansen[b,**,2], Pepper Schedin[a,f,g,*,2]

[a] Department of Cell, Developmental and Cancer Biology, Oregon Health & Science University, Portland, OR, USA
[b] Department of Biochemistry and Molecular Genetics, University of Colorado Anschutz Medical Campus, Aurora, CO, USA
[c] Department of Surgery, Center for Bioengineering and Tissue Regeneration, University of California San Francisco, San Francisco, CA, USA
[d] Department of Medicine, Division of Medical Oncology, University of Colorado Anschutz Medical Campus, Aurora, CO, USA
[e] University of Colorado Cancer Center, Aurora, CO, USA
[f] Young Women's Breast Cancer Translational Program, University of Colorado Anschutz Medical Campus, Aurora, CO, USA
[g] Knight Cancer Institute, Oregon Health & Science University, Portland, OR, USA

ARTICLE INFO

Article history:
Received 1 April 2016
Received in revised form 15 October 2016
Accepted 18 October 2016
Available online 24 October 2016

Keywords:
Extracellular matrix
Mass spectrometry proteomics
Mammary gland
Liver
Breast cancer
Liver metastasis

ABSTRACT

Normal epithelium exists within a dynamic extracellular matrix (ECM) that is tuned to regulate tissue specific epithelial cell function. As such, ECM contributes to tissue homeostasis, differentiation, and disease, including cancer. Though it is now recognized that the functional unit of normal and transformed epithelium is the epithelial cell and its adjacent ECM, we lack a basic understanding of tissue-specific ECM composition and abundance, as well as how physiologic changes in ECM impact cancer risk and outcomes. While traditional proteomic techniques have advanced to robustly identify ECM proteins within tissues, methods to determine absolute abundance have lagged. Here, with a focus on tissues relevant to breast cancer, we utilize mass spectrometry methods optimized for absolute quantitative ECM analysis. Employing an extensive protein extraction and digestion method, combined with stable isotope labeled Quantitative conCATamer (QconCAT) peptides that serve as internal standards for absolute quantification of protein, we quantify 98 ECM, ECM-associated, and cellular proteins in a single analytical run. In rodent models, we applied this approach to the primary site of breast cancer, the normal mammary gland, as well as a common and particularly deadly site of breast cancer metastasis, the liver. We find that mammary gland and liver have distinct ECM abundance and relative composition. Further, we show mammary gland ECM abundance and relative compositions differ across the reproductive cycle, with the most dramatic changes occurring during the pro-tumorigenic window of weaning-induced involution. Combined, this work suggests ECM candidates for investigation of breast cancer progression and metastasis, particularly in postpartum breast cancers that are characterized by high metastatic rates. Finally, we suggest that with use of absolute quantitative ECM proteomics to characterize tissues of interest, it will be possible to reconstruct more relevant in vitro models to investigate tumor-ECM dynamics at higher resolution.

1. Introduction

Mechanistic studies of rodent mammary gland development reveal requisite roles for ECM in mammary epithelial cell proliferation, differentiation, and cell-death decisions (Aggeler et al., 1988; Streuli et al., 1991; Werb et al., 1996; Fata et al., 2004; Schedin et al.,

Abbreviations: CNBr, cyanogen bromide; DAVID, Database for Annotation Visualization and Integrated Discovery; ECM, extracellular matrix; EHS, Engelbreth Holm-Swarm; FACIT, fibril-associated collagens with interrupted triple helices; FASP, filter assisted sample prep; iECM, insoluble ECM; IHC, immunohistochemistry; LC–MS/MS, liquid chromatography–tandem mass spectrometry; LC-SRM, liquid chromatography-selected reaction monitoring; MG, mammary gland; PCA, principle component analysis; PLS-DA, partial least squares discriminate analysis; PTM, post-translational modification; QC, quality control; QconCAT, quantitative conCATamer; sECM, soluble ECM; SIL, stable isotope labeled.

* Corresponding author at: Mail Code L215, 3181 SW Sam Jackson Park Rd., Oregon Health & Science University, Portland, OR 97239-3098, USA.
** Corresponding author.

E-mail addresses: kirk.hansen@ucdenver.edu (K.C. Hansen), schedin@ohsu.edu (P. Schedin).
[1] These authors contributed equally to this work.
[2] Corresponding authors contributed equally to this work.

http://dx.doi.org/10.1016/j.biocel.2016.10.014

2004; Nelson et al., 2006). In fact, pioneering investigations identified the functional unit of the epithelium as the cell plus its adjacent ECM (Bissell and Barcellos-Hoff, 1987; Barcellos-Hoff et al., 1989). These findings shifted studies aimed at understanding epithelial cell function from a cell-intrinsic to a cell-stroma focus (Howlett and Bissell, 1993). Investigation of the relationship between tissue ECM and epithelium has also been applied to the study of breast cancer, with important gains (Weigelt et al., 2014).

The functions of matrix proteins in breast cancer have been assessed primarily using single, purified ECM proteins or by admixing ECM proteins of interest with commercially available Engelbreth-Holm Swarm (EHS) matrix that is enriched in laminin-111 (Shaw et al., 2004; Lee et al., 2007; Fischbach et al., 2007; Krause et al., 2008). Such studies identified specific ECM protein-integrin interactions, matrix stiffness, and matrix architecture as critical mediators of tumor cell function (Schmeichel et al., 1998; DuFort et al., 2011; Schedin and Keely, 2011; Levental et al., 2009). Single ECM molecules, including collagen I, fibronectin, and tenascin-C, display clear roles in promoting tumor cell proliferation, motility, and invasion (Levental et al., 2009; Hancox et al., 2009; Maity et al., 2011; Nguyen-Ngoc et al., 2012; Maller et al., 2013). ECM roles in breast cancer risk are also suggested, as high mammographic breast density, indicative of elevated collagen content in the breast, increases epithelial cell transformation by 4–6-fold (Boyd et al., 1998; Li et al., 2005). The relationship between fibrillar collagen I and cancer incidence and progression have been corroborated in rodent models, where high collagen I content in the murine mammary gland results in a ~3-fold increase in tumor formation as well as increased lung metastasis (Provenzano et al., 2008). There is also evidence that distinct ECM proteins at secondary sites of metastasis impact metastatic success (Barkan et al., 2010; Erler et al., 2009; Oskarsson et al., 2011; Malanchi et al., 2012; Ghajar et al., 2013; Costa-Silva et al., 2015; Kaplan et al., 2005; Burnier et al., 2011; Goto et al., 2015). In particular, prominent work in the metastasis field has shown roles for lung and liver fibronectin in supporting disseminated tumor cell seeding and growth in murine models of colon, mammary, and pancreatic adenocarcinomas (Costa-Silva et al., 2015; Kaplan et al., 2005). Cumulatively, these studies implicate ECM in all stages of cancer progression, from initiation to metastatic outgrowth at secondary sites.

The reductionist approach of investigating single ECM protein-cell interactions *in vitro*, or manipulating single proteins *in vivo*, while revealing, does not replicate the complex ECM milieu of an *in vivo* tissue microenvironment. One example of the importance of tissue-specific ECM is found in rodent models of postpartum breast cancer. In these models, whole tissue mammary ECM, as opposed to a single protein, has been shown to determine metastatic outcomes (McDaniel et al., 2006). Relevance to women is implicated, as postpartum breast cancer patients have a ~3-fold increased risk for metastasis and death (Callihan et al., 2013; Johansson et al., 2011; Stensheim et al., 2009), a poor prognosis attributed, in part, to ECM remodeling during postpartum breast involution (Schedin, 2006). Specifically, weaning-induced mammary gland involution is characterized by deposition and partial proteolysis of radially aligned fibrillar collagen, fibronectin, and tenascin-C (McDaniel et al., 2006; Lyons et al., 2011). Further, evidence that involution-specific mammary ECM promotes metastasis has been demonstrated in xenograft models. Tumor cells co-injected with mammary ECM isolated from involuting glands grew larger tumors within the mammary fat pad and metastasized at much higher rate compared to tumor cells co-injected with mammary ECM isolated from nulliparous rats (McDaniel et al., 2006). These data highlight the need to better understand how physiologic cues as well as disease states impact ECM composition and abundance, and provide compelling rationale for developing improved quantitative methodologies for ECM proteomics.

Robust characterization of tissue-specific ECM complexity and abundance has been largely hindered by technical challenges in the field of proteomics. For unbiased biochemical identification of proteins, mass spectrometry provides a highly sensitive approach. However, improvements to proteomic approaches for the study of tissue-specific ECM have been hindered by the proteolytic- and solubilization-resistant properties of ECM proteins, which are often high molecular weight, extensively glycosylated, and covalently cross-linked. While significant advances in ECM protein identification have occurred recently (Naba et al., 2014a,b; Hansen et al., 2009; Didangelos et al., 2010), proteomics approaches still largely fail to adequately quantify many ECM proteins despite their high abundance in tissues (Hill et al., 2015). We have recently established methods for improved tissue solubilization and absolute protein quantification to interrogate tissue-specific ECM. This approach permits quantitative assessment of a subset of ECM proteins that represent >99% of spectra matching to core ECM and ECM-affiliated proteins identified in mammary gland and liver by global proteomics (Hill et al., 2015; Baiocchini et al., 2016; Geiger et al., 2013). To gain insight into primary breast cancer and site-specific metastasis, we utilize our quantitative proteomics approach to compare rat mammary gland and liver, as the liver is a common and lethal site of breast cancer metastasis. We also investigate ECM composition and abundance changes in the mammary gland across a reproductive cycle. Our objective was to gain insight into potential roles of ECM in the pro- tumorigenic window of weaning-induced mammary gland involution. This targeted ECM proteomics approach is anticipated to facilitate improved *in vivo* characterization, and *in vitro* reconstruction of epithelial cell microenvironments for use in cancer, stem cell, and regenerative biology.

2. Materials and methods

2.1. Rodent studies

The OHSU Institutional Animal Care and Use Committees approved all animal procedures. Sprague-Dawley female rats (Harlan), 70 +/−3 days of age, were bred and tissues collected as described (Schedin et al., 2004; Bemis and Schedin, 2000). Snap frozen, pulverized lymph node-free mammary gland [n = 5/group for nulliparous, late pregnancy (day 18–21), lactation, involution days 2, 4, 6, 8, and 10, and four weeks post-weaning (regressed)] and gallbladder-free liver [n = 6 for nulliparous] were used for ECM-based QconCAT proteomic analyses. Pooled samples generated from the above mentioned biologic replicates were utilized for global proteomics.

2.2. Imaging

Tissue H&E and trichrome stains were scanned on an Aperio ScanScope AT, image analysis was performed using Aperio ImageScope software (Leica Biosystems).

2.3. Sample preparation for proteomic analysis

Approximately 5 and 50 mgs of fresh frozen mammary gland and liver, respectively, was pulverized in liquid nitrogen and processed as described (Hill et al., 2015). Briefly, tissue samples were homogenized in CHAPS buffer with 2 mm glass beads using mechanical agitation (Bullet Blender®, Next Advance) on power 8 for 3 min. Following homogenization, tissue samples were sequentially extracted using high-speed centrifugation after vortexing in high salt CHAPS buffer, 6 M urea, and CNBr buffers resulting in 3 fractions for each sample: (1) cellular fraction, (2) soluble ECM,

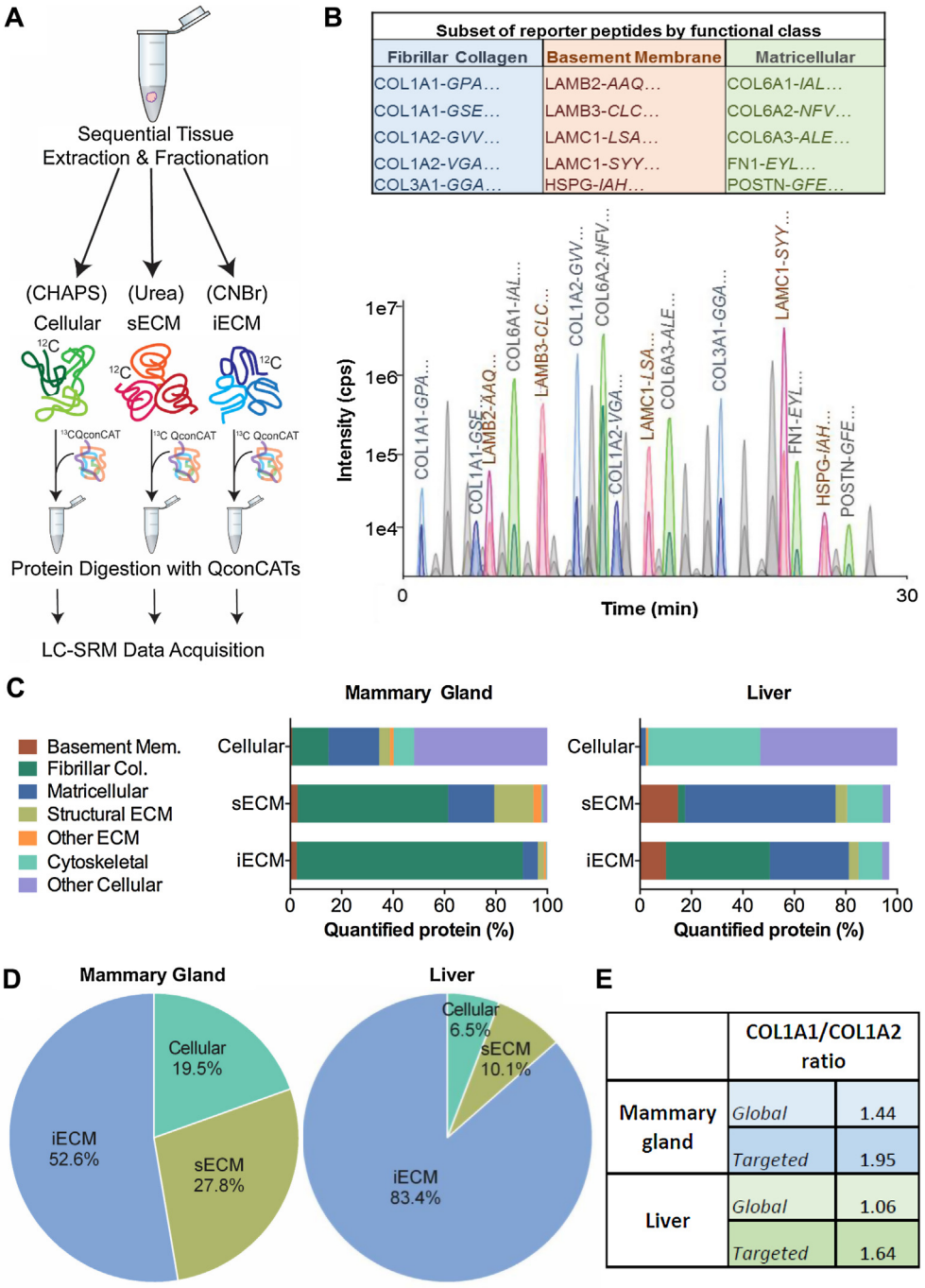

Fig 1. Quantitative QconCAT ECM proteomics pipeline.
A) Experimental pipeline for quantitative ECM proteomics. Tissues are sequentially extracted to obtain cellular, soluble ECM (sECM), and insoluble ECM (iECM) fractions. QconCATs are spiked into fractions and samples are then proteolytically digested (full list of Quantitative conCATamers in Supplementary Table 1). B) Table of a subset of the 98 ECM/ECM-associated proteins represented in the Quantitative conCATamers (QconCAT) used to determine absolute concentration of proteins by mass spectrometry proteomics; the first three amino acids of the peptide represented are identified in italics (top). Representative chromatographic elution profile of equal molar concentration of conCATamer peptides detected by LC-SRM mass spectrometry demonstrates peptide-specific spectral profiles (bottom). For labeled peaks, darker shading indicates $^{12}C_6$ peptide (endogenous) and lighter shading indicates $^{13}C_6$ peptide (QconCAT), which is spiked in at known, equimolar concentrations. Integrated peak areas are used for ratio metric determination of endogenous peptide levels, a surrogate for protein concentration (bottom). C) Percent of proteins identified within the cellular, sECM, and iECM fractions of rat mammary gland (left) and liver (right) according to the DAVID gene ontology functional group classification. D) Percent of collagen I identified in cellular, sECM, and iECM fractions of rat mammary gland (left) and liver (right). E) Ratio of collagen alpha-1(I) to collagen alpha-2(I) for peptide spectral matches vs. QconCAT based quantification in rat mammary gland and liver.

and (3) insoluble ECM (Figure 1A). All fractions were ran by liquid chromatography-tandem mass spectrometry (LC–MS/MS) and liquid chromatography-selected reaction monitoring (LC-SRM). LC-SRM analysis was done on n = 5 mammary gland/group and n = 6 liver samples, with n = 7 technical replicates. LC–MS/MS analysis was done on pooled biological replicates for an n = 1/group.

2.4. Detergent/chaotrope removal & protein digestion

Sample cleanup and protein digestion was carried out as described (Johnson et al., 2016). QconCAT standards were spiked into each sample prior to filter assisted sample prep (FASP) to yield values of 100 fmol $^{13}C_6$ QconCAT/5 μg of protein for LC-SRM injections. Equal volumes of biological replicates were combined for LC–MS/MS analysis.

2.5. Liquid chromatography tandem mass spectrometry & data analysis

Samples were analyzed by LC-SRM and LC–MS/MS as described (Johnson et al., 2016). Equal volumes from each post-digestion sample were combined and injected every third run and used to monitor technical reproducibility. Skyline was used for method development and to extract the ratio of endogenous light peptides to heavy internal standards from LC- SRM data for protein quantification as described (MacLean et al., 2010). LC–MS/MS data was processed as previously described (Hill et al., 2015). Limits of detection, quantification, and dynamic range were determined for each peptide as previously described (Hill et al., 2015) and provided in Supplementary Table 1. Principal component analysis (PCA) and partial least squares discriminate analysis (PLS-DA) were calculated using the MetaboAnalyst online platform (Xia et al., 2015).

2.6. Statistics

Statistical analysis was performed using GraphPad Prism 6. Comparison of two groups was done by two-sided Student's T-test. Comparison of >two groups was done using One-way ANOVA.

3. Results

3.1. Development of quantitative ECM proteomic methodology

To better understand the complexity of epithelial cell-ECM microenvironments *in vivo*, we developed novel extraction and digestion methods for proteomic characterization of ECM (Hansen et al., 2009; Hattar et al., 2009; O'Brien et al., 2012). While these methodological advancements have furthered our understanding of ECM composition, they lacked the ability to accurately quantify ECM protein abundance in the microenvironment. To overcome this barrier, we designed six recombinantly generated Quantitative conCATamers (QconCAT) (Hill et al., 2015; Pratt et al., 2006) made of 201 stable isotope labeled (SIL) peptides representing 98 ECM, ECM-associated, and common cellular proteins (Supplementary Table 1). Peptides specific to intracellular proteins from different subcellular locations were included to serve as a quality control measure for development of tissue extraction methods and as a relative measure of cellularity. These reporter peptides are then 'spiked into' experimental protein lysates at equimolar concentrations to serve as internal quantitation controls. Fig. 1A shows a schematic representation of the tissue extraction/fractionation, and digestion workflows used prior to LC-SRM data acquisition. Our fractionation protocol yields three distinct fractions, cellular, soluble ECM (sECM), and insoluble ECM (iECM). The iECM fraction is then treated with cyanogen bromide (CNBr) to increase solubility. Reporter ECM peptides are added to all fractions, and samples are proteolytically digested and run by LC-SRM. The consolidated results from the three fractions yield total quantity for a given protein within a tissue. This targeted mass spectrometry method allows us to measure all 201 SIL QconCAT peptides and endogenous analogs in a single 30 min analytical run. Molecular heterogeneity can differentially affect signal intensity during LC-SRM data acquisition, which is why the inclusion of internal standardized controls for each unique protein of interest is essential for determining accurate absolute concentrations. We find the QconCAT generated heavy peptides allow for precise quantification, as the reporter peptides behave identically to the endogenous peptides in terms of mass spectrometry fragmentation and ionization, chromatographic separation, and enzymatic digestion efficiency (Fig. 1B).

To confirm increased detection of rat mammary and liver ECM proteins with this method, the protein identifications within the 3 fractions (cellular, sECM, and iECM) were grouped into functional classifications of cytoskeletal, other cellular, matricellular, and several ECM categories, using gene ontology terminology from the Database for Annotation, Visualization, and Integrated Discovery (DAVID) (Dennis et al., 2003). The vast majority of mammary cellular proteins fractionate with CHAPS detergent into the cellular fraction, whereas sECM and iECM fractions were highly enriched for ECM proteins (Fig. 1C). In the rat liver, we again found that the majority of cellular proteins resolved with CHAPS. The liver sECM fraction was enriched for matricellular proteins and the iECM fraction further enriched for fibrillar collagens (Fig. 1C). Strikingly, 52% of mammary and 83% of liver collagen I was detected in the iECM fraction after CNBr treatment (Fig. 1D), a fraction not routinely incorporated into traditional proteomic methods. Additionally, other residual ECM proteins failed to completely solubilize with urea (sECM fraction), highlighting the importance of CNBr solubilization and analysis of the iECM fraction (Fig. 1C). The utility of using our targeted reporter peptide approach compared to a global proteomics approach is further realized by analyzing the ratio of collagen alpha-1(I) to collagen alpha-2(I) by LC-SRM. The expected stoichiometry between these two chains is 2:1 (COL1A1/COL1A2), based on the assembly of fibrillar collagen triple helices containing two alpha-1 chains and one alpha-2 chain. We find that the targeted approach with QconCATs more accurately reflects the theoretical ratio of 2:1 than a traditional global proteomics approach (Fig. 1E).

3.2. QconCAT based proteomics reveals unique and shared mammary gland and liver ECM profiles

A major rate-limiting step of metastatic success has been attributed to discordance between the ECM requirements of the seeding tumor cell and the ECM microenvironment at the secondary site (Barkan et al., 2010; Oskarsson et al., 2011; Malanchi et al., 2012; Costa-Silva et al., 2015; Luzzi et al., 1998). In the context of breast cancer, we utilized our quantitative ECM proteomics to begin to address this hypothesis by elucidating tissue-specific differences as well as similarities between the primary and liver metastatic site in the nulliparous female adult rat. We focused on the liver, as one of three common sites of breast cancer metastasis (Berman et al., 2013; Savci-Heijink et al., 2015; Harrell et al., 2012), which confers the worst prognosis (Wyld et al., 2003; Tarhan et al., 2013; Tseng et al., 2013). The resulting proteomic data were grouped into 10 functional classifications of proteins including: basement membrane, ECM regulator, fibril-associated collagens with interrupted triple helices (FACIT) collagen, fibrillar collagen, matricellular, other ECM, secreted ECM, and structural ECM, using DAVID, as described in Fig. 1 (Dennis et al., 2003). This analysis demonstrated an abundance of fibrillar collagens and matricellular proteins in mammary tissue, and high levels of cytoskeletal and other cellular proteins in liver (Fig. 2A, Supplementary Tables 2 and 3), data consistent with the high stromal and low epithelial content in the mammary gland as compared to the liver (Fig. 2B). Further, these tissues differed markedly in overall ECM abundance, with ~100 nmol of ECM per gram of tissue in the mammary gland compared to ~8.5 nmol/g in the liver (Fig. 2C).

To further interrogate ECM complexity and abundance of ECM proteins between the mammary gland and the liver, we removed cellular proteins from the assessment. This ECM- biased analysis

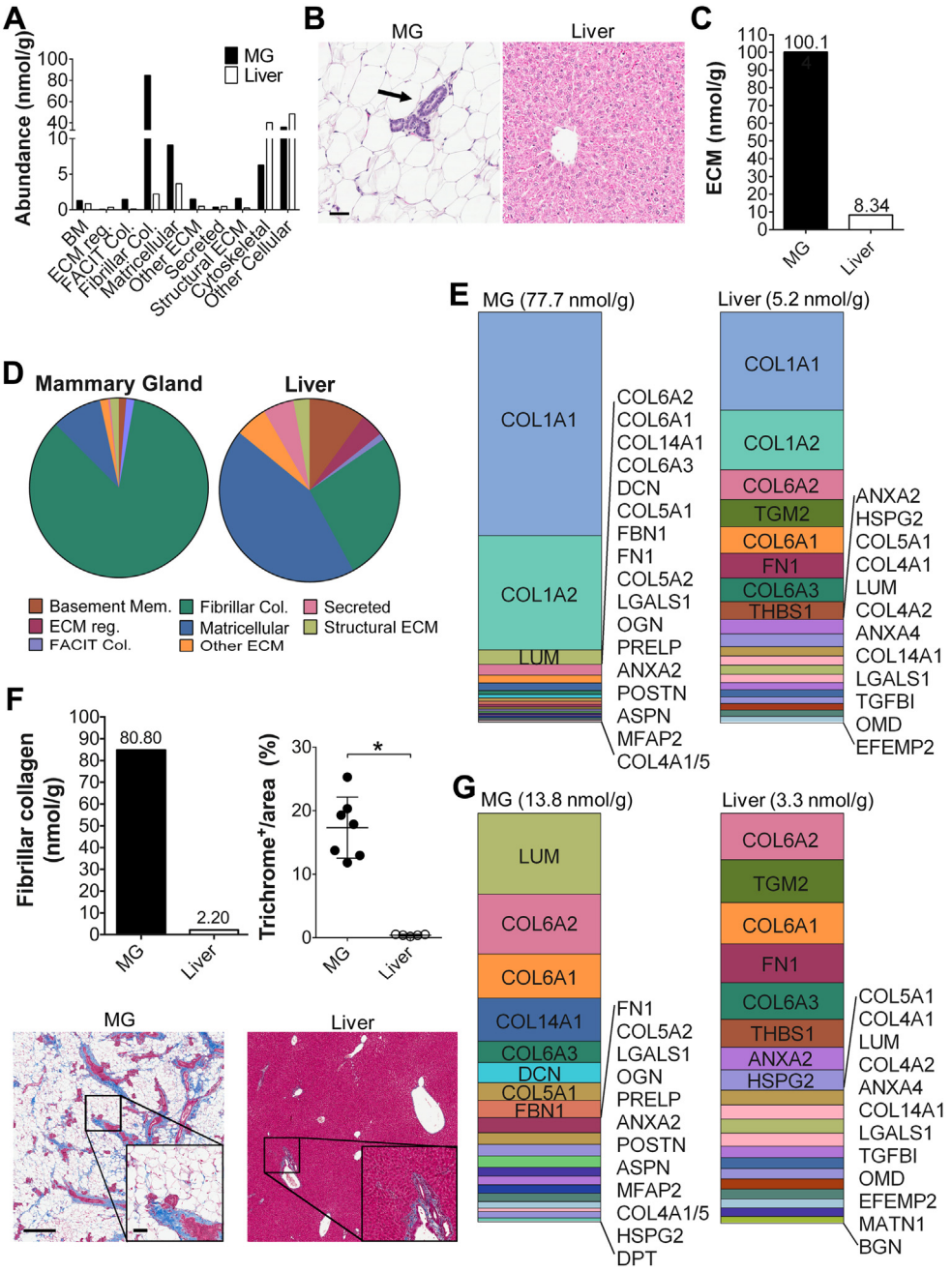

Fig. 2. QconCAT based ECM proteomics reveals unique mammary gland and liver ECM profiles.
A) QconCAT based ECM proteomics of nulliparous rat mammary gland and liver tissues displayed as total abundance of proteins (nmol/g of tissue) grouped by DAVID gene ontology functional classifications; n = 5 rats/group for mammary gland and n = 6 rats for liver analyses. B) Representative H&E stained rat mammary gland (MG; left) and liver (right) showing tissue specific differences in stromal-epithelial cell composition; scale bar = 60 μm (arrow = MG epithelium; liver H&E shows epithelium throughout the tissue). C) Nanomolar concentration of total ECM per gram of tissue from QconCAT proteomics in the mammary gland and liver. D) Abundance of ECM and ECM-associated proteins based on DAVID gene ontology functional groups with cytoskeletal and cellular protein groups excluded. E) Twenty most abundant ECM proteins in the rat MG (left) and liver (right) as detected by QconCAT proteomics. Tabular results in Supplementary Tables 2 & 3. F) Nanomolar concentration of fibrillar collagen in MG and liver from QconCAT proteomic analysis (top left) and collagen trichrome staining quantification in MG and liver (top right). Representative trichrome stained images (blue stain) of rat MG (bottom left) and liver (bottom right); scale bar = 250 μm, inset scale bar = 60 μm. * = p-value < 0.0001, Student's T-test. G) Twenty most abundant ECM proteins, excluding collagen I, in the rat MG (left) and liver (right) as detected by QconCAT proteomics, tabular results shown in Supplementary Tables 2 & 3.

revealed that nulliparous mammary gland ECM is >80% fibrillar collagen, ~9% matricellular proteins, 1.3% basement membrane proteins, and ~5% combined FACIT collagens and structural, regulatory, secreted and other ECMs (Fig. 2D). In contrast, in the liver, matricellular proteins make up 44% of ECM proteins, followed by 26.4% fibrillar collagen, ~10% basement membrane, and 15.3% combined FACIT collagens and structural, regulatory, secreted and other ECMs (Fig. 2D). Although the absolute concentration of fibrillar collagen is vastly different between mammary gland and liver, fibrillar collagen I remains the most abundant single ECM protein in both tissues (Fig. 2E), providing further support for an essential role of collagen I in tissue structure and homeostasis (Mouw et al., 2014). Our observed molar concentrations of fibrillar collagens in mammary gland and liver (Fig. 2F, upper left panel) correlate with relative fibrillar collagen abundance detected by trichrome stain

(Fig. 2F, upper right panel and representative images), reinforcing potential biologic relevance of the QconCAT method.

To investigate ECM complexity beyond fibrillar collagen I, we stratified QconCAT data based on the next twenty most abundant ECM proteins (Fig. 2G, highlighted in Supplementary Tables 2 and 3). Despite the concentration of ECM in the mammary gland dropping significantly with removal of collagen I, ECM concentration of the remaining twenty proteins was still ~4-fold higher in the mammary gland compared to liver (Fig. 2E, G). Overall, we identified the same ECM proteins in both the mammary gland and liver, however, their relative ratios were tissue specific (Fig. 2G). For example, lumican, collagen VI, and collagen XIV were prevalent in the mammary gland and collagen VI and fibronectin were prevalent in liver (Fig. 2G). Further, we find that while fibronectin is present at ~equimolar concentrations in the mammary gland and liver (Supplementary Fig. 1), it makes up only 0.64% of total ECM concentration in the mammary gland compared to 4.74% in the liver (Fig. 2G, Supplementary Tables 2 & 3). The absolute quantitation method also permits the identification of a subset of ECM proteins, including thrombospondin 1 and fibulin 4, that are present at significantly higher concentrations in liver, in spite of the mammary gland having ~12-fold higher concentration of total ECM (Supplementary Fig. 1). In sum, these analyses demonstrate the ability of the QconCAT method to provide absolute molar concentrations of specific ECM proteins within the mammary gland and liver and identify tissue-specific ECM complexity.

3.3. *Mammary gland ECM proteomics across the reproductive cycle*

The microenvironment of the mammary gland can be neutral, tumor- promotional, or tumor-suppressive, dependent upon reproductive state (Maller et al., 2013; Martinson et al., 2014), a phenomenon thought to be driven in large part by reproductive state-dependent changes to mammary ECM (Maller et al., 2013; Schedin et al., 2004; Lyons et al., 2011). Specifically, in rodent models of breast cancer, mammary tumor cells grow most robustly in the weaning-induced involuting microenvironment, moderately in the nulliparous mammary microenvironment, and least when transplanted into parous mice, whose mammary glands have completed weaning-induced involution (Maller et al., 2013; Martinson et al., 2014). Despite this dynamic fluctuation in tumor-supportive function, mammary ECM has never been assessed across the reproductive cycle using quantitative proteomics. To this end, we analyzed rat mammary ECM in whole gland lysates from nulliparous, pregnancy, lactating, involuting (i.e., 2, 4, 6, 8 and 10 days post-weaning), and fully involuted (regressed) stages. Principle component analysis (PCA) on LC-SRM data generated from these ECM proteomics data revealed a cycle of mammary gland ECM remodeling across pregnancy, lactation and involution, upon which the gland ultimately returns to an ECM microenvironment similar to, but distinct from, the nulliparous state (Fig. 3 & Supplementary Fig. 2). We observed a >2-fold drop in ECM abundance when comparing nulliparous to pregnancy, lactation, and involution day 2 stages (Fig. 4A), data consistent with the increased epithelial cellularity as well as loss of collagen staining at these reproductive stages (Schedin et al., 2004). Total ECM abundance increased to pre-pregnant levels by involution day 6, consistent with epithelial cell loss and stromal repopulation upon weaning (Lund et al., 1996). We also observed increased abundance of ECM in the fully regressed mammary gland compared to the nulliparous host, data suggestive of unique mammary microenvironments in nulliparous and parous hosts (Fig. 4A), and consistent with previous reports (Maller et al., 2013).

We next compared the top twenty most abundant ECM proteins in the mammary glands from nulliparous, involution days 2 and 6,

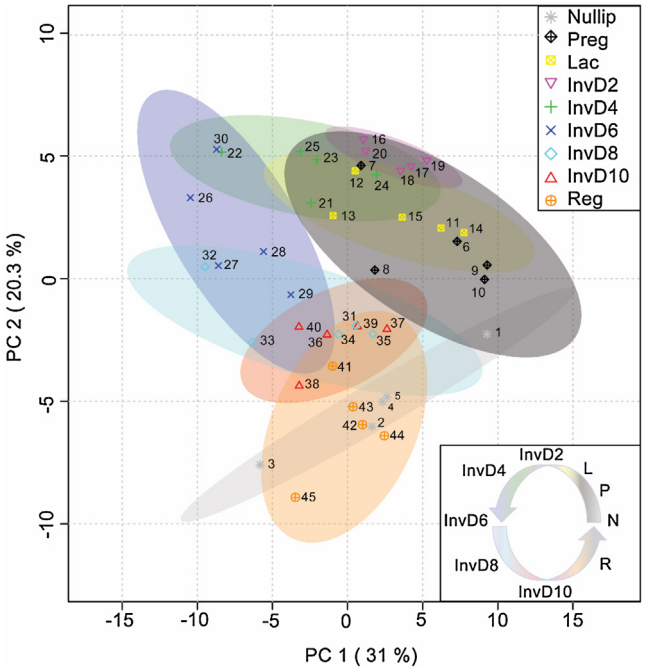

Fig. 3. Quantitative ECM proteomics reveals dynamic and cyclical mammary gland ECM remodeling across the reproductive cycle.
Principle component analysis of quantitative ECM proteomics performed on rat mammary glands across the reproductive cycle (Nullip = nulliparous; Preg = pregnancy days 18–21; Lac = lactation day 10; InvD2-InvD10 = involution days 2, 4, 6, 8, and 10; Reg = regressed, 4 weeks post- weaning); n = 5 rats/grp. Data shows that ECM composition in the mammary gland changes in phase with the reproductive cycle in a stepwise, cyclical fashion.

and regressed stages, since these stages have differential tumor-promotional attributes (Maller et al., 2013; Martinson et al., 2014). We confirmed that collagen I is the predominant ECM protein in the gland (Hansen et al., 2009; O'Brien et al., 2012), and extended these analyses to demonstrate that collagen abundance is dramatically reduced during pregnancy, and does not return to high levels until 6 days post-weaning (Fig. 4A and B). To investigate ECM complexity further, we removed collagen I from the analysis and found a high abundance of lumican, collagen VI, and collagen XIV in the nulliparous and regressed rat mammary gland (Fig. 4C and D & Supplementary Table 2). In contrast to these relatively quiescent mammary glands, actively involuting glands exhibited a prominent abundance of collagen VI, thrombospondin 1, and galectin-3 (Fig. 4C and D). Two additional ECM proteins not found in the top twenty list, tenascin-C and collagen XII, also increased in abundance during mammary gland involution (Fig. 4D). Intriguingly, the ECM composition of the involuting mammary gland somewhat resembles that of the liver, which share increased collagen VI and fibronectin, and reduced lumican and collagen I abundances (Fig. 2G and C). Principle component analysis confirmed tissue specificity of liver and mammary ECM, but also revealed that liver ECM resembles the mammary gland at pregnancy, lactation, and involution days 2 and 4, compared to other reproductive stages (Supplementary Fig. 3). Taken together, these data highlight how quantitative ECM proteomics can provide prime candidates for the investigation of the roles of ECM in breast cancer progression.

4. Discussion

This work describes advances made in sample preparation techniques and quantitative proteomics methods for the study of tissue ECM composition and abundance. Using this experimental pipeline, we characterized tissue-specific ECM composition of the rodent

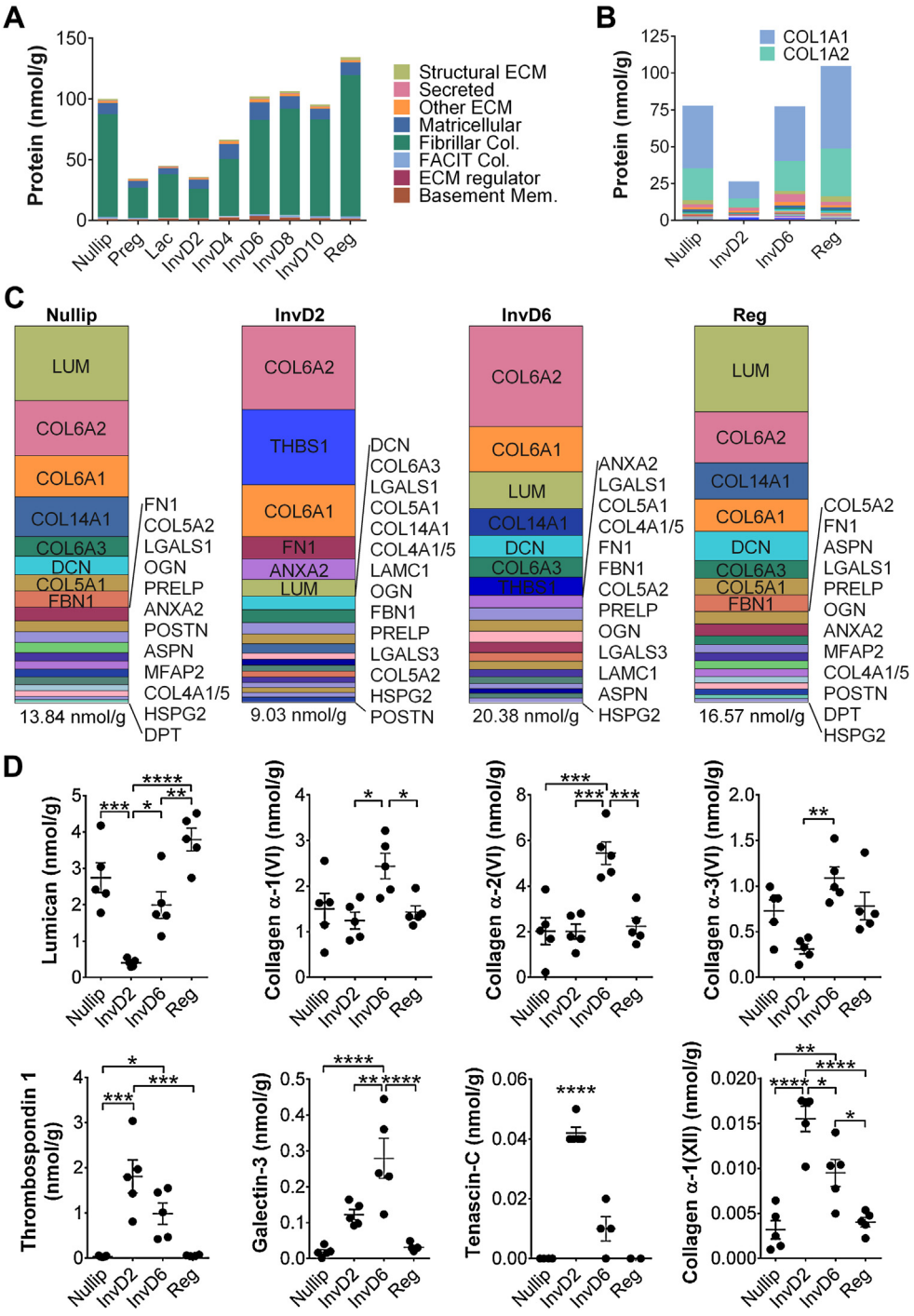

Fig. 4. Quantitative ECM proteomics unravels the unique composition and abundance of ECM proteins across the reproductive cycle.
QconCAT based ECM proteomics of rat MG tissues across the reproductive cycle, with identified cellular protein groups removed; n = 5 rats/grp. B) Twenty most abundant ECM proteins in Nullip, InvD2, InvD6, and Reg stage rat MG; tabular results highlighted in Supplementary Table 2. C) Twenty most abundant ECM proteins in Nullip, InvD2, InvD6, and Reg stage rat MG, with collagen I removed from the analysis. Tabular results in Supplementary Table 2. D) Select tumor suppressive (lumican) and tumor- promotional (collagen VI, thrombospondin 1, galectin-3, tenascin-C) ECM protein levels, as well as collagen XII from individual rats, as determined by QconCAT based ECM proteomics of Nullip, InvD2, InvD6, and Reg stages, n = 5 rats/grp; * = p-value < 0.05, ** = p-value < 0.01, *** = p-value < 0.001, **** = p-value < 0.0001, One-way ANOVA.

mammary gland and liver, a lethal site of breast cancer metastasis, to a level not previously accomplished. These analyses identified putative tissue-specific ECM components, including lumican and collagen XIV, which were prevalent in the mammary gland, and fibronectin which was prevalent in the liver. We also found shared ECM components between these two tissues, including abundant proteins such as collagen types I and VI, as well as less abundant collagen types IV and V. We also show that the abundance of mammary gland ECM is altered across the reproductive cycle, building upon previous studies that have identified major shifts in mammary ECM with pregnancy, lactation, involution, and regression (Schedin et al., 2004; Lyons et al., 2011; Bemis and Schedin, 2000; O'Brien et al., 2010). In particular, we see elevated abundance of known pro- tumorigenic ECM proteins collagen VI, thrombospondin 1, galectin-3, and tenascin-C during weaning- induced mammary gland involution. Further, to the best of our knowledge, we iden-

tify collagen XII for the first time as elevated during post-weaning mammary involution. Importantly, potential roles for each of these highlighted ECM proteins in breast cancer metastasis have been elucidated, with the exception of collagen XII (Iyengar et al., 2005; Ioachim et al., 2002; Yee et al., 2009; Zhang et al., 2014). While collagen XII has been shown to be upregulated in malignant breast cancer cell lines, and has been identified as a prognostic marker in other cancers, its role in breast cancer progression has yet to be established (Karagiannis et al., 2012; Yen et al., 2014). In sum, our data demonstrate tissue-specific ECM complexity and ECM protein stoichiometry between the mammary gland and liver, and across a reproductive cycle within the mammary gland, data consistent with ECM contributing to differential tissue function.

Somewhat surprisingly, we also found that the ECM profile of the early involuting mammary gland (InvD2-InvD4) resembled that of the liver. This finding may provide insight into site-specific metastasis of postpartum breast cancers, as disseminated tumor cells may experience a survival advantage if primary and secondary sites have similar ECM compositions post- weaning. A prediction of these data are increased risk for liver metastasis in postpartum breast cancer patients; a relationship that remains unexplored. Of potential relevance, risk for liver metastasis is elevated in younger breast cancer patients (Cummings et al., 2014), a significant proportion of whom are likely to be postpartum breast cancer patients (Callihan et al., 2013).

Our quantitative QconCAT ECM proteomics approach facilitates in-depth characterization of tissue-specific ECM abundance and composition at a level not previously attained. The advances we report result, in part, from improved solubilization using a CNBr extraction step that permits detection of historically insoluble ECM proteins such as collagen I. Further, the use of in-house generated QconCATs for quantification of tissue ECM proteins has several advantages over traditional relative quantitative approaches, including 1) SIL peptide mimics that control for matrix effects during proteomic acquisition, allowing for direct comparison between heterogeneous tissues, 2) inclusion of full-length QconCATs during digestion, which control for sample loss and digestion variability, and 3) absolute quantitative values allowing for inter-protein and -experiment comparisons between samples. However, as with any first-generation experimental pipeline, there are limitations to the methodology that need to be addressed in future work. First, targeted proteomics is inherently more specific and therefore will only quantitate peptides/proteins included in the QconCAT library. However, when comparing our current QconCAT library coverage to samples simultaneously run using global proteomics, only an additional 7 and 8 ECM proteins (primarily Annexins, accounting for 0.43% and 0.11% of total spectral matches) were identified that were not covered by the QconCAT library. Further, QconCAT proteomics quantified 34 and 41 proteins or protein isoforms in the mammary gland and liver, respectively, not identified by global proteomics (Supplementary Table 4). These comparisons highlight the benefits of increased sensitivity when applying a targeted proteomics approach, as this level of detection often requires deep fractionation and multiple runs to achieve similar depth using global proteomics.

An additional caveat to QconCAT proteomics is that quantification of endogenous peptides with post-translational modifications (PTMs) is not currently possible. We circumvent this problem by designing QconCAT peptides specific to proteins that either have no known PTMs or do not contain a common PTM motif so that the quantified endogenous peptide has a higher probability of representing the molar equivalent of the protein it represents. Furthermore, we attempt to include multiple peptides per protein of interest to account for splice variants, known PTMs, and matricryptic sites, however a subset of proteins are currently covered by only a single peptide. Future generations of this QconCAT library will increase confidence in protein quantification by expanding coverage of ECM, ECM-modifying, and ECM-associated proteins, as well as adding additional peptides for all ECM protein targets. Importantly, the increased depth of ECM coverage that will be gained by design of additional QconCATs will ultimately facilitate more refined characterization of ECM abundance and composition in tissues.

Multiple studies have characterized both the mammary gland and liver in a variety of normal and tumorigenic contexts (Naba et al., 2014a, 2014b; Baiocchini et al., 2016; Geiger et al., 2013; Lai et al., 2008, 2011; Da Costa et al., 2015; Moreira et al., 2010). However, because these semi-quantitative approaches provide relative, and not absolute abundance of proteins, it is difficult to compare data across studies. For example, comparison of collagen coverage in the liver across our platform and five published datasets revealed marked variability between both identification and quantification of collagen (Supplementary Table 5). While the majority of datasets identified the abundant collagens I & VI, they varied dramatically in estimated abundance and in the identification of less abundant collagens. Significant differences in estimated abundance of collagen I between studies are likely derived from variability in enrichment strategies, and the non-uniform analysis of insoluble collagens in the iECM pellet, a protein fraction not routinely captured in standard proteomics pipelines (Hill et al., 2015). The quantitative advantage of QconCATs is apparent with comparison of collagen alpha-1(I) to collagen alpha-2(I) ratios, as our targeted approach recapitulated the expected 2:1 ratio (Fig. 1E & Supplementary Table 5). Additionally, collagen alpha- 1/2/3(VI) organizes into a 1:1:1 heterotrimer (Chu et al., 1990), and again, our study is the only one to reveal such a distribution (Supplementary Table 5). The level of variability across proteomics datasets highlights the need for standardization, and suggest that solubilization with CNBr along with absolute quantification may provide additional biological relevance to proteomics pipelines focused on ECM proteins.

To the best of our knowledge, our ECM-based QconCAT proteomics pipeline has provided the most quantitative assessment of ECM proteins and tissue composition in mammary gland and liver to date. In the future, the application of this method can be utilized to more fully interrogate breast cancer progression. For example, a comparison of young women's breast tumors and paired metastases, similar to work done by Naba et al. in colorectal cancer (Naba et al., 2014a), is predicted to reveal widespread ECM differences and further inform our understanding of breast cancer metastasis. Further, studies to understand liver, as well as lung, bone, and brain ECM throughout the reproductive cycle may shed insight into site-specific metastasis in premenopausal breast cancer patients. The impact of the ECM biased proteomic pipeline could be further realized in the context of regenerative medicine, where understanding the composition of ECM components and the relative stoichiometry within specific organs would be critical steps in accurately recapitulating endogenous matrices. Ultimately, compilation of similar datasets for additional organs would lay the foundation for an ECM Atlas that would be capable of comparing absolute quantitative measurements between all organs, facilitating a broader understanding of the role of ECM in physiology and pathology.

5. Conclusions

ECM can be quantitatively analyzed from tissues under diverse physiologic and pathologic conditions using the improved solubilization and quantitative proteomics methodologies presented here. We report tissue-specific ECM signatures in rat liver compared to mammary gland, as well as diverse ECM complexity and abundance in the rat mammary gland throughout a reproductive cycle. These studies provide novel avenues to elucidate how ECM

impacts breast cancer progression, particularly postpartum breast cancer. Our quantitative ECM proteomics approach has broad applicability and can be utilized in studies pertaining to various tissue and disease sites, treatment responses, stem cell biology, and tissue regeneration.

Author contributions

KH, VFB and PS were responsible for hypothesis development, conceptual design and final data integrity and interpretation. RCH, AB, and KH developed proteomics methodology and performed all proteomic analyses. OM, CBB, QG, and ETG performed rat studies. RCH, AB, and ETG performed mammary gland and liver proteomic data analyses. All authors contributed to the conceptual design of the manuscript and to data interpretation. ETG, RCH, and PS wrote the manuscript and all authors edited and approved the final manuscript submission.

Acknowledgements

The authors would like to acknowledge Jacob Fischer for assisting with experimental metastasis studies, Hadley Holden for performing special stains, and Weston Anderson for providing editorial review of the manuscript. Monika Dzieciatkowska assisted with QconCAT generation and validation. Finally, the work included in this manuscript includes funding from NIH/NCI NRSAF31CA186524 (to ETG), NIH/NCATS Colorado CTSIUL1 TR001082 for proteomic support, NIH/NCIR33CA183685 (to KH), DODBC123567 (to PS), BC123567P1 (to KH), and NIH/NCI 5R01CA169175 (to VB and PS). The authors declare no competing financial interests.

Appendix A. Supplementary data

Supplementary data associated with this article can be found, in the online version, at http://dx.doi.org/10.1016/j.biocel.2016.10.014.

References

Aggeler, J., Park, C.S., Bissell, M.J., 1988. Regulation of milk protein and basement membrane gene expression: the influence of the extracellular matrix. J. Dairy Sci. 71, 2830–2842.
Baiocchini, A., et al., 2016. Extracellular matrix molecular remodeling in human liver fibrosis evolution. PLoS One 11, e0151736.
Barcellos-Hoff, M.H., Aggeler, J., Ram, T.G., Bissell, M.J., 1989. Functional differentiation and alveolar morphogenesis of primary mammary cultures on reconstituted basement membrane. Dev. (Cambridge, Engl.) 105, 223–235.
Barkan, D., et al., 2010. Metastatic growth from dormant cells induced by a col-I-enriched fibrotic environment. Cancer Res. 70, 5706–5716.
Bemis, L.T., Schedin, P., 2000. Reproductive state of rat mammary gland stroma modulates human breast cancer cell migration and invasion. Cancer Res. 60, 3414–3418.
Berman, A.T., Thukral, A.D., Hwang, W.T., Solin, L.J., Vapiwala, N., 2013. Incidence and patterns of distant metastases for patients with early-stage breast cancer after breast conservation treatment. Clin. Breast Cancer 13, 88–94.
Bissell, M.J., Barcellos-Hoff, M.H., 1987. The influence of extracellular matrix on gene expression: is structure the message? J. Cell Sci. Suppl. 8, 327–343.
Boyd, N.F., et al., 1998. Mammographic densities and breast cancer risk. Breast Dis. 10, 113–126.
Burnier, J.V., et al., 2011. Type IV collagen-initiated signals provide survival and growth cues required for liver metastasis. Oncogene 30, 3766–3783.
Callihan, E.B., et al., 2013. Postpartum diagnosis demonstrates a high risk for metastasis and merits an expanded definition of pregnancy-associated breast cancer. Breast Cancer Res. Treat. 138, 549–559.
Chu, M.L., et al., 1990. The structure of type VI collagen. Ann. N. Y. Acad. Sci. 580, 55–63.
Costa-Silva, B., et al., 2015. Pancreatic cancer exosomes initiate pre-metastatic niche formation in the liver. Nat. Cell Biol. 17, 816–826.
Cummings, M.C., et al., 2014. Metastatic progression of breast cancer: insights from 50 years of autopsies. J. Pathol. 232, 23–31.
Da Costa, G.G., et al., 2015. Comparative proteomics of tumor and paired normal Breast tissue highlights potential biomarkers in Breast cancer. Cancer Genom. Proteom. 12, 251–261.
Dennis Jr., G., et al., 2003. DAVID: database for annotation, visualization, and integrated discovery. Genome Biol. 4, P3.
Didangelos, A., et al., 2010. Proteomics characterization of extracellular space components in the human aorta. Mol. Cell. Proteom. 9, 2048–2062.
DuFort, C.C., Paszek, M.J., Weaver, V.M., 2011. Balancing forces: architectural control of mechanotransduction. Nat. Rev. Mol. Cell Biol. 12, 308–319.
Erler, J.T., et al., 2009. Hypoxia-induced lysyl oxidase is a critical mediator of bone marrow cell recruitment to form the premetastatic niche. Cancer Cell 15, 35–44.
Fata, J.E., Werb, Z., Bissell, M.J., 2004. Regulation of mammary gland branching morphogenesis by the extracellular matrix and its remodeling enzymes. Breast Cancer Res.: BCR 6, 1–11.
Fischbach, C., et al., 2007. Engineering tumors with 3D scaffolds. Nat. Methods 4, 855–860.
Geiger, T., et al., 2013. Initial quantitative proteomic map of 28 mouse tissues using the SILAC mouse. Mol. Cell. Proteom. 12, 9–1722.
Ghajar, C.M., et al., 2013. The perivascular niche regulates breast tumour dormancy. Nat. Cell Biol. 15, 807–817.
Goto, R., Nakamura, Y., Takami, T., Sanke, T., Tozuka, Z., 2015. Quantitative LC–MS/MS analysis of proteins involved in metastasis of Breast cancer. PLoS One 10, e0130760.
Hancox, R.A., et al., 2009. Tumour-associated tenascin-C isoforms promote breast cancer cell invasion and growth by matrix metalloproteinase-dependent and independent mechanisms. Breast Cancer Res. 11, R24.
Hansen, K.C., et al., 2009. An in-solution ultrasonication-assisted digestion method for improved extracellular matrix proteome coverage. Mol. Cell. Proteom. 8, 1648–1657.
Harrell, J.C., et al., 2012. Genomic analysis identifies unique signatures predictive of brain, lung, and liver relapse. Breast Cancer Res. Treat. 132, 523–535.
Hattar, R., et al., 2009. Tamoxifen induces pleiotrophic changes in mammary stroma resulting in extracellular matrix that suppresses transformed phenotypes. Breast Cancer Res. 11, R5.
Hill, R.C., Calle, E.A., Dzieciatkowska, M., Niklason, L.E., Hansen, K.C., 2015. Quantification of extracellular matrix proteins from a rat lung scaffold to provide a molecular readout for tissue engineering. Mol. Cell. Proteom.
Howlett, A.R., Bissell, M.J., 1993. The influence of tissue microenvironment (stroma and extracellular matrix) on the development and function of mammary epithelium. Epithelial Cell Biol. 2, 79–89.
Ioachim, E., et al., 2002. Immunohistochemical expression of extracellular matrix components tenascin, fibronectin, collagen type IV and laminin in breast cancer: their prognostic value and role in tumour invasion and progression. Eur. J. Cancer 38, 2362–2370.
Iyengar, P., et al., 2005. Adipocyte-derived collagen VI affects early mammary tumor progression in vivo, demonstrating a critical interaction in the tumor/stroma microenvironment. J. Clin. Invest. 115, 1163–1176.
Johansson, A.L., Andersson, T.M., Hsieh, C.C., Cnattingius, S., Lambe, M., 2011. Increased mortality in women with breast cancer detected during pregnancy and different periods postpartum. Cancer Epidemiol. Biomark. Prev. 20, 1865–1872.
Johnson, T.D., et al., 2016. Quantification of decellularized human myocardial matrix: a comparison of six patients. Proteom. Clin. Appl. 10, 75–83.
Kaplan, R.N., et al., 2005. VEGFR1-positive haematopoietic bone marrow progenitors initiate the pre-metastatic niche. Nature 438, 0820–827.
Karagiannis, G.S., et al., 2012. Proteomic signatures of the desmoplastic invasion front reveal collagen type XII as a marker of myofibroblastic differentiation during colorectal cancer metastasis. Oncotarget 3, 267–285.
Krause, S., Maffini, M.V., Soto, A.M., Sonnenschein, C., 2008. A novel 3D in vitro culture model to study stromal-epithelial interactions in the mammary gland. Tissue Eng. Part C Methods 14, 261–271.
Lai, K.K., Kolippakkam, D., Beretta, L., 2008. Comprehensive and quantitative proteome profiling of the mouse liver and plasma. Hepatology 47, 1043–1051.
Lai, K.K., et al., 2011. Extracellular matrix dynamics in hepatocarcinogenesis: a comparative proteomics study of PDGFC transgenic and Pten null mouse models. PLoS Genet. 7, e1002147.
Lee, G.Y., Kenny, P.A., Lee, E.H., Bissell, M.J., 2007. Three- dimensional culture models of normal and malignant breast epithelial cells. Nat. Methods 4, 359–365.
Levental, K.R., et al., 2009. Matrix crosslinking forces tumor progression by enhancing integrin signaling. Cell 139, 891–906.
Li, T., et al., 2005. The association of measured breast tissue characteristics with mammographic density and other risk factors for breast cancer. Cancer Epidemiol. Biomark. Prev. 14, 343–349.
Lund, L.R., et al., 1996. Two distinct phases of apoptosis in mammary gland involution: proteinase-independent and -dependent pathways. Development 122, 181–193.
Luzzi, K.J., et al., 1998. Multistep nature of metastatic inefficiency: dormancy of solitary cells after successful extravasation and limited survival of early micrometastases. Am. J. Pathol. 153, 865–873.
Lyons, T.R., et al., 2011. Postpartum mammary gland involution drives progression of ductal carcinoma in situ through collagen and COX-2. Nat. Med. 17, 1109–1115.
MacLean, B., et al., 2010. Skyline: an open source document editor for creating and analyzing targeted proteomics experiments. Bioinformatics 26, 966–968.
Maity, G., et al., 2011. Culture of human breast cancer cell line (MDA-MB-231) on fibronectin-coated surface induces pro-matrix metalloproteinase-9 expression and activity. Tumour Biol. 32, 129–138.

Malanchi, I., et al., 2012. Interactions between cancer stem cells and their niche govern metastatic colonization. Nature 481, 85–89.
Maller, O., et al., 2013. Collagen architecture in pregnancy-induced protection from breast cancer. J. Cell Sci. 126, 4108–4110.
Martinson, H.A., Jindal, S., Durand-Rougely, C., Borges, V.F., Schedin, P., 2014. Wound healing-like immune program facilitates postpartum mammary gland involution and tumor progression. Int. J. Cancer.
McDaniel, S.M., et al., 2006. Remodeling of the mammary microenvironment after lactation promotes breast tumor cell metastasis. Am. J. Pathol. 168, 608–620.
Moreira, J.M., et al., 2010. Tissue proteomics of the human mammary gland: towards an abridged definition of the molecular phenotypes underlying epithelial normalcy. Mol. Oncol. 4, 539–561.
Mouw, J.K., Ou, G., Weaver, V.M., 2014. Extracellular matrix assembly: a multiscale deconstruction. Nat. Rev. Mol. Cell Biol. 15, 771–785.
Naba, A., et al., 2014a. Extracellular matrix signatures of human primary metastatic colon cancers and their metastases to liver. BMC Cancer 14, 518.
Naba, A., Clauser, K.R., Lamar, J.M., Carr, S.A., Hynes, R.O., 2014b. Extracellular matrix signatures of human mammary carcinoma identify novel metastasis promoters. Elife 3, e01308.
Nelson, C.M., Vanduijn, M.M., Inman, J.L., Fletcher, D.A., Bissell, M.J., 2006. Tissue geometry determines sites of mammary branching morphogenesis in organotypic cultures. Sci. (New York, N.Y.) 314, 298–300.
Nguyen-Ngoc, K.V., et al., 2012. ECM microenvironment regulates collective migration and local dissemination in normal and malignant mammary epithelium. Proc. Natl. Acad. Sci. U. S. A. 109, E2595–E2604.
O'Brien, J., et al., 2010. Alternatively activated macrophages and collagen remodeling characterize the postpartum involuting mammary gland across species. Am. J. Pathol. 176, 1241–1255.
O'Brien, J.H., Vanderlinden, L.A., Schedin, P.J., Hansen, K.C., 2012. Rat mammary extracellular matrix composition and response to ibuprofen treatment during postpartum involution by differential GeLC–MS/MS analysis. J. Proteome Res. 11, 4894–4905.
Oskarsson, T., et al., 2011. Breast cancer cells produce tenascin C as a metastatic niche component to colonize the lungs. Nat. Med. 17, 867–874.
Pratt, J.M., et al., 2006. Multiplexed absolute quantification for proteomics using concatenated signature peptides encoded by QconCAT genes. Nat. Protoc. 1, 1029–1043.
Provenzano, P.P., et al., 2008. Collagen density promotes mammary tumor initiation and progression. BMC Med. 6, 11.
Savci-Heijink, C.D., et al., 2015. Retrospective analysis of metastatic behaviour of breast cancer subtypes. Breast Cancer Res. Treat. 150, 547–557.
Schedin, P., Keely, P.J., 2011. Mammary gland ECM remodeling, stiffness, and mechanosignaling in normal development and tumor progression. Cold Spring Harb. Perspect. Biol. 3, a003228.
Schedin, P., Mitrenga, T., McDaniel, S., Kaeck, M., 2004. Mammary ECM composition and function are altered by reproductive state. Mol. Carcinog. 41, 207–220.
Schedin, P., 2006. Pregnancy- associated breast cancer and metastasis. Nat. Rev. Cancer 6, 281–291.
Schmeichel, K.L., Weaver, V.M., Bissell, M.J., 1998. Structural cues from the tissue microenvironment are essential determinants of the human mammary epithelial cell phenotype. J. Mammary Gland Biol. Neoplasia 3, 201–213.
Shaw, K.R., Wrobel, C.N., Brugge, J.S., 2004. Use of three-dimensional basement membrane cultures to model oncogene-induced changes in mammary epithelial morphogenesis. J. Mammary Gland Biol. Neoplasia 9, 297–310.
Stensheim, H., Moller, B., van Dijk, T., Fossa, S.D., 2009. Cause- specific survival for women diagnosed with cancer during pregnancy or lactation: a registry-based cohort study. J. Clin. Oncol. 27, 45–51.
Streuli, C.H., Bailey, N., Bissell, M.J., 1991. Control of mammary epithelial differentiation: basement membrane induces tissue-specific gene expression in the absence of cell–cell interaction and morphological polarity. J. Cell Biol. 115, 1383–1395.
Tarhan, M.O., et al., 2013. The clinicopathological evaluation of the breast cancer patients with brain metastases: predictors of survival. Clin. Exp. Metastasis 30, 201–213.
Tseng, L.M., et al., 2013. Distant metastasis in triple-negative breast cancer. Neoplasma 60, 290–294.
Weigelt, B., Ghajar, C.M., Bissell, M.J., 2014. The need for complex 3D culture models to unravel novel pathways and identify accurate biomarkers in breast cancer. Adv. Drug Deliv. Rev. 69–70, 42–51.
Werb, Z., et al., 1996. Extracellular matrix remodeling and the regulation of epithelial-stromal interactions during differentiation and involution. Kidney Int. 54, S68–74.
Wyld, L., et al., 2003. Prognostic factors for patients with hepatic metastases from breast cancer. Br. J. Cancer 89, 284–290.
Xia, J., Sinelnikov, B., Wishart, D.S., 2015. MetaboAnalyst 3. 0 – making metabolomics more meaningful. Nucleic Acids Res. 43, W251–W257.
Yee, K.O., et al., 2009. The effect of thrombospondin-1 on breast cancer metastasis. Breast Cancer Res. Treat. 114, 85–96.
Yen, T.Y., et al., 2014. Using a cell line breast cancer progression system to identify biomarker candidates. J. Proteom. 96, 173–183.
Zhang, H., et al., 2014. Galectin-3 as a marker and potential therapeutic target in breast cancer. PLoS One 9, e103482.